How to cite: *Angew. Chem. Int. Ed.* **2022,** *61,* e202117807
International Edition: doi.org/10.1002/anie.202117807
German Edition: doi.org/10.1002/ange.202117807

MOFs

Self-Adjusting Metal–Organic Framework for Efficient Capture of Trace Xenon and Krypton

Zheng Niu, Ziwen Fan, Tony Pham, Gaurav Verma, Katherine A. Forrest, Brian Space, Praveen K. Thallapally,* Abdullah M. Al-Enizi, and Shengqian Ma**

Abstract: *The capture of the xenon and krypton from nuclear reprocessing off-gas is essential to the treatment of radioactive waste. Although various porous materials have been employed to capture Xe and Kr, the development of high-performance adsorbents capable of trapping Xe/Kr at very low partial pressure as in the nuclear reprocessing off-gas conditions remains challenging. Herein, we report a self-adjusting metal-organic framework based on multiple weak binding interactions to capture trace Xe and Kr from the nuclear reprocessing off-gas. The self-adjusting behavior of ATC-Cu and its mechanism have been visualized by the in-situ single-crystal X-ray diffraction studies and theoretical calculations. The self-adjusting behavior endows ATC-Cu unprecedented uptake capacities of 2.65 and 0.52 mmol g^{-1} for Xe and Kr respectively at 0.1 bar and 298 K, as well as the record Xe capture capability from the nuclear reprocessing off-gas. Our work not only provides a benchmark Xe adsorbent but proposes a new route to construct smart materials for efficient separations.*

Pursuing the balance between energy demand and the environment is an emerging issue in our generation.[1] Albeit confronted with some negative criticisms, nuclear power generation has prevented about 1.84 million air pollution-related deaths and reduced CO_2 emissions by 64 billion tons from supplementing fossil fuels.[2] The rapid growth of nuclear industries has generated tons of associated high-level radioactive waste which must be safely sequestered; otherwise it would cause serious environmental issues.[3] In the treatment of nuclear fuel wastes, gaseous radioactive krypton and xenon are difficult to capture compared with other species.[4] For gaseous radioactive krypton and xenon, the long half-life of ^{85}Kr ($t_{1/2} \approx 10.8$ years) urges its separation and capture from the off-gas to avoid radioactive contamination, while the radioactive ^{135}Xe can capture a neutron to transmute to stable ^{136}Xe, which can be used in the field from lighting, laser, medical imaging to anaesthesia.[5] Furthermore, the capture of Xe in the treatment of nuclear fuel waste can significantly lower the price of the Xe since the concentration of Xe in the nuclear fission gas is 4500 times higher than in the atmosphere.[6] Currently, cryogenic distillation technology is mostly used to separate Xe and Kr from nuclear reprocessing off-gas,[7] which is energy-intensive and uneconomic.

Alternatively, porous materials can capture Xe and Kr from nuclear reprocessing off-gas with greater energy efficiency. Among various types of porous materials, metal-organic frameworks (MOFs) exhibit superior Xe and Kr capture performance[8] compared to porous organic cage compounds and traditional porous materials including silver-loaded zeolites and activated carbons.[9] Reported MOFs for capturing Xe and Kr can be grouped as a) rigid framework, which exhibits no significant structural change after gas filling (Scheme 1A); and b) flexible framework, which exhibits profound structural change after gas filling (Scheme 1B). The rigid framework with appropriately sized pore can accommodate the Xe/Kr atoms[10] but the fine-tuning of pore size is not an easy task. Some flexible MOFs

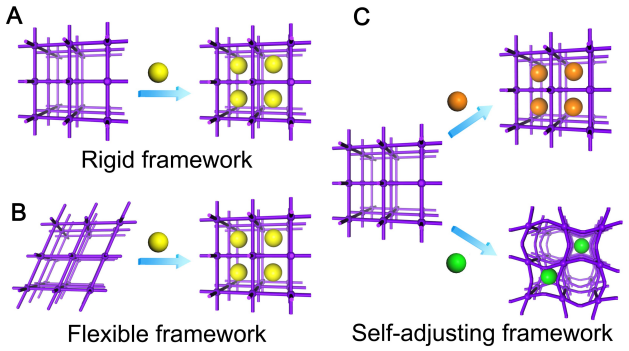

Scheme 1. The illustrative structures of the A) rigid, B) flexible, and C) self-adjusting frameworks.

[*] Prof. Z. Niu, Z. Fan
College of Chemistry, Chemical Engineering and Materials Science
Soochow University, Suzhou 215123 (P.R. China)
E-mail: zhengniu@suda.edu.cn
Dr. G. Verma, Prof. S. Ma
Department of Chemistry, University of North Texas
Denton, TX 76201 (USA)
E-mail: Shengqian.Ma@unt.edu
P. K. Thallapally
Physical and Computational Science Directorate
Pacific Northwest National Laboratory, Richland, WA 99354 (USA)
E-mail: praveen.thallapally@pnnl.gov
Dr. T. Pham, Dr. K. A. Forrest
Department of Chemistry, University of South Florida
4202 E. Fowler Avenue, Tampa, FL 33620 (USA)
Prof. B. Space
Department of Chemistry, North Carolina State University
2700 Stinson Dr., Raleigh, NC 27607 (USA)
Prof. A. M. Al-Enizi
Department of Chemistry, College of Science, King Saud University
Riyadh 11451 (Saudi Arabia)

show the breathing effects after filling with Xe or Kr molecules and thus realize the separation of Xe and Kr.[11] However, since the breathing effect has the threshold concentration to the target gas, it is difficult to be applied to the capture of trace amounts of Xe and Kr.

In this work, we proposed a self-adjusting framework to capture trace Xe and Kr from the nuclear reprocessing off-gas. As illustrated in Scheme 1C, different from the rigid framework and flexible framework, the pores of the self-adjusting framework can smartly adjust their pore size for the target gases, and remain unchanged for other gases. In this regard, we choose an alkyl porous MOF, anhydrous Cu_2(ATC) (denoted by ATC-Cu),[12] which has a semi-rigid framework and includes two types of hydrogen-rich cavities. The framework of ATC-Cu can adjust its pores to accommodate the target gases (Xe/Kr) yet remain unresponsive to the main gases of nuclear reprocessing off-gas (N_2 and O_2) at normal pressure and temperature. Taking advantage of the self-adjusting behavior, ATC-Cu demonstrates the record Xe and Kr uptake capacity at 0.1 bar and 298 K, as well as the benchmark Xe capture capability in the nuclear reprocessing off-gas.

ATC-Cu was synthesized according to the literature with minor modifications (See Supporting Information). As shown in Figure 1A, four Cu paddle-wheel secondary building units (SBUs) were connected by the ATC ligand to construct a 4,4-coordinated net. The framework of ATC-Cu includes Cu-open metal sites and two types of hydrogen-rich polyhedron cavities, Cavity I (green) and Cavity II (purple). The midpoint of C_4 axis of Cavity I and the symmetry center of Cavity II are defined as the centers of Cavity I and II, respectively. The average distance between the center and the atom on the vertex of the polyhedron cavity (denoted as $(C\text{-}V)_{av}$ hereafter) is 3.90 Å and 3.85 Å for Cavity I and II, respectively. Cavity I has eight H atoms and eight oxygen atoms, while Cavity II has twelve H atoms (Figure 1B). The powder X-ray diffraction (PXRD) pattern of the as-synthesized ATC-Cu sample agrees well with the calculated pattern from the single crystal data. Furthermore, the thermogravimetric analysis (TGA) data revealed that ATC-Cu is stable till 270 °C. The Brunauer–Emmett–Teller (BET) surface area of ATC-Cu is about 600 $m^2 g^{-1}$ (Langmuir surface area: 667 $m^2 g^{-1}$), which was calculated from the N_2 sorption isotherms at 77 K.

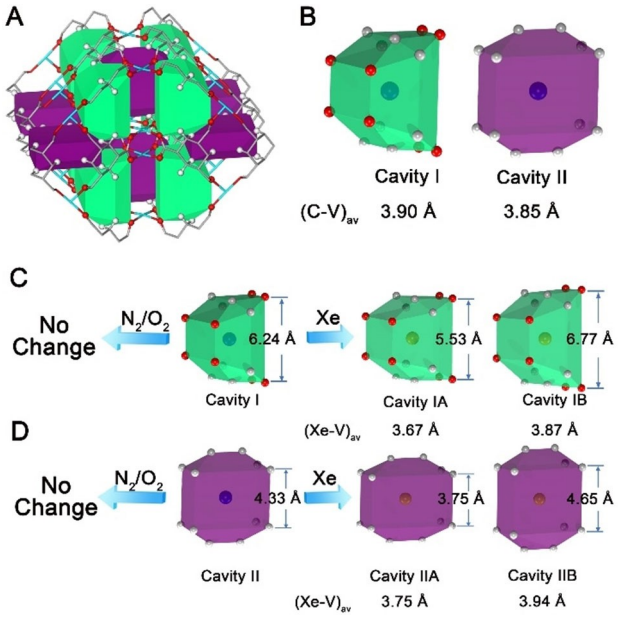

Figure 1. A) The cavities in the framework of ATC-Cu. B) The enlarged view of Cavity I and II. The change of the Cavity I (C) and Cavity II (D) after adsorbing N_2, O_2, and Xe. (The blue ball in Cavity I and II stand for the center of the cavities, and the gold ball in Cavity IA, IB, IIA and IIB stand for the SCXRD determined location of Xe in ATC-Cu).

The gas-loaded single-crystal X-ray diffraction (SCXRD) experiments were performed to detect the impact of N_2, O_2, Xe, and Kr on the ATC-Cu framework.[13] After exposing into N_2 or O_2 atmosphere at 298 K and 1 bar for 12 h, the cavities in ATC-Cu remain unchanged, indicating that the framework of ATC-Cu shows rigidity toward N_2 and O_2 presumably due to the very weak interactions. However, after loading Xe to ATC-Cu under the same conditions, significant changes of the ATC-Cu framework were observed. Different from the O_2 and N_2 molecules, the relatively stronger interaction between Xe and H/O atoms on the cavities of ATC-Cu make the parts of the cavities in the ATC-Cu framework can shrink and smartly fit Xe atoms, and the rest cavities in the framework are enlarged to balance the inner stress of the crystal. As shown in Figure 1C and D, Xe atoms are located at the center of the cavities or nearby. Compared with $(C\text{-}V)_{av}$ of Cavity I, the average distance between Xe and the atoms (denoted as $(Xe\text{-}V)_{av}$ hereafter) on Cavity IA and IIA decreases from 3.90 Å to 3.67 Å and 3.75 Å respectively. Meanwhile, the shape of the Cavity IA and IB exhibits the significant changes: the length of Cavity I changes from 6.24 Å to 5.53 Å and 6.77 Å for Cavity IA and IB respectively (Figure 1C). The similar self-adjusting behavior can also be observed at Cavity IB and IIB, yet the $(Xe\text{-}V)_{av}$ of Cavity IIB increases from 3.85 Å ($(C\text{-}V)_{av}$ of Cavity II) to 3.94 Å (Figure 1D). Although the uptake amount of Kr in ATC-Cu is less than that of Xe, we also can observe the Kr atoms lead the change of length of cavities, which indicates that the similar interactions as Xe (Scheme S1). Consequently, ATC-Cu exhibits the self-adjusting behavior for Xe and Kr, while exhibiting unresponsive to N_2 and O_2. The above self-adjusting behavior may be attributed to the interactions between Xe/Kr atoms and framework caused local dynamics.

Further studies of the Xe and Kr loaded ATC-Cu crystals revealed the mechanism of the self-adjusting behavior in ATC-Cu. As presented in Figure 2, there are four primary locations of Xe atoms in ATC-Cu, which are based on multiple C–H···Xe interactions. Remarkably, although the site between two opposite Cu paddle-wheel exhibits excellent CH_4 and C_2H_2 adsorption capability,[14] a few Xe or Kr atoms can be observed at the site from in-situ SCXRD. The above results suggest the Cu unsaturated metal site is not the preferred Xe or Kr adsorption site. To explore the preferential Xe adsorption site, we employed periodic

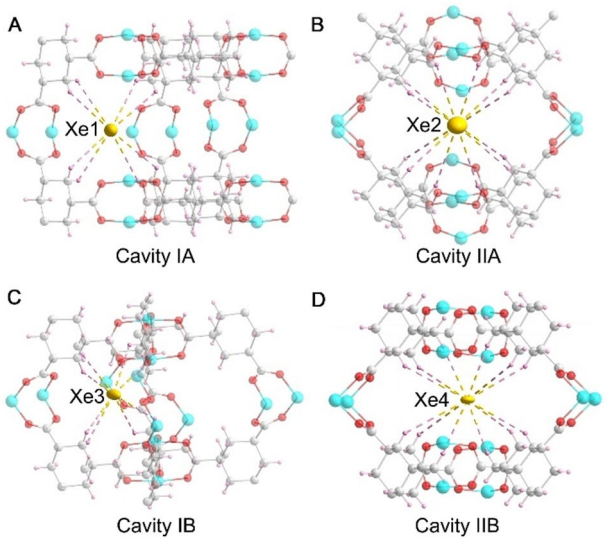

Figure 2. The in-situ SCXRD determined locations of Xe atoms in the cavities of ATC-Cu.

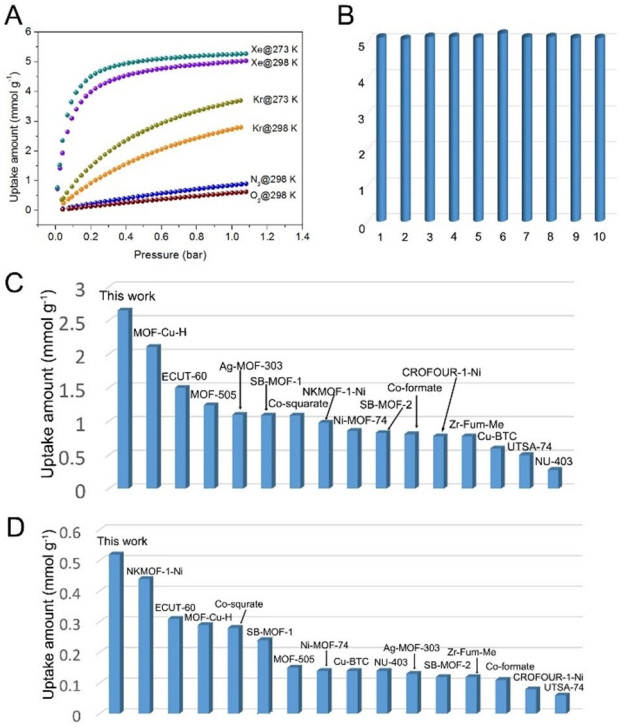

Figure 3. A) The Xe, Kr, O_2, and N_2 isotherms for ATC-Cu; B) Xe adsorption/desorption cycling data of ATC-Cu. Survey of Xe (C) and Kr uptake amount (D) at 298 K and 0.1 bar in ATC-Cu and other top-performance materials.

density functional theory (DFT) methods to determine the absolute energies for different Xe adsorption sites in ATC-Cu as revealed through SCXRD. The calculation results indicated that the contractive cavities, Cavity IA and IIA, are the energetically favorable sites in ATC-Cu, with the calculated energy of 39.38 and 41.56 kJ mol^{-1} for Xe1 and Xe2, while the expanded Cavity IB and IIB exhibits the lower energy of 37.45 and 31.28 kJ mol^{-1}, which are much lower than the contractive cavities. The calculation results further confirmed the self-adjusting behavior of ATC-Cu is caused by the synergistic effect based on multiple weak interactions between Xe and the framework. Calculations of the adsorption energies for Kr adsorbed about the analogous sites in ATC-Cu revealed notably lower binding energies compared to those for Xe (Table S10).

To investigate the impact of the self-adjusting behavior on the gas adsorption capability of ATC-Cu, the single-component adsorption isotherms for Xe, Kr, N_2, and O_2 were collected at 298 K. As illustrated in Figure 3A, the uptake amounts of N_2 and O_2 for ATC-Cu is significantly lower than Xe and Kr. The Xe uptake capacity of ATC-Cu reaches 2.65 mmol g^{-1} at 298 K and 0.1 bar, compared favorably with the reported porous materials[8,10,11] (Figure 3C). Similarly, Kr uptake amount of ATC-Cu at 298 K respectively attains 2.7 and 0.52 mmol g^{-1} at 1 and 0.1 bar, which are the record values under similar conditions[8,10,11] (Figure 3D). Upon reaching 1 bar at 298 K, ATC-Cu can adsorb 5.0 mmol g^{-1} or 0.95 g cm^{-3} Xe, which is even higher than xenon hydrate (0.85 g cm^{-3}). Furthermore, ATC-Cu exhibits excellent cycle performance; as shown in Figure 3B, the uptake amount of Xe exhibits no decrease after ten cycles. The excellent Xe and Kr capability at low pressures and room temperatures suggests that ATC-Cu is a promising material for Xe and Kr capture even in the ambient atmosphere.

Inspired by the significant difference in the uptake amount between Xe/Kr and N_2/O_2 in ATC-Cu, the selectivity of Xe/N_2 and Xe/O_2 as well as the uptake amount of Xe in the mixture gas (400 ppm Xe, balanced by N_2 or O_2) was determined using the Ideal Adsorbed Solution Theory (IAST). Meanwhile, the selectivity of Kr/N_2 and Kr/O_2 as well as the uptake amount of Kr in the mixture gas (1000 ppm Kr, balanced by N_2 or O_2) at 298 K and 1 bar was also determined by IAST. As displayed in Figure S7 and S8, the calculated Xe/N_2 and Xe/O_2 selectivity for the corresponding mixture gas (400 ppm Xe, balanced by N_2 or O_2) in ATC-Cu are 66 and 109 respectively at 298 K and 1 bar. For 400 ppm Xe in N_2 and 1000 ppm Kr in N_2, the calculated uptake amount attains to 22.2 mmol kg^{-1} and 4.2 mmo kg^{-1}, respectively. Furthermore, the selectivity of Xe/Kr was also determined using IAST. The Xe/Kr selectivity for the Kr/Xe mixture (Xe/Kr = 20/80 v/v) is 13.9, which is lower than Co-squarate, SB-MOF-1, CROFOUR-1-Ni, and MOF-Cu-H, but higher than other MOFs (Table S4).[8,10,11]

Given the high selectivity of Xe and Kr over N_2 and O_2 calculated by IAST, the column breakthrough experiments were performed with a gas mixture consisting of 400 ppm Xe, 40 ppm Kr balanced with N_2 and O_2. This condition is present in the nuclear reprocessing industry and any material that is capable to selectively separate Xe and Kr over the other gases, near room temperature, would potentially replace cryogenic technology. Therefore, column breakthrough experiments at room temperature on Cu-ATC were performed, by feeding air with 400 ppm Xe and 40 ppm Kr and monitored using a mass spectrometer as shown in Figure 4A. The retention time of Xe is longer than

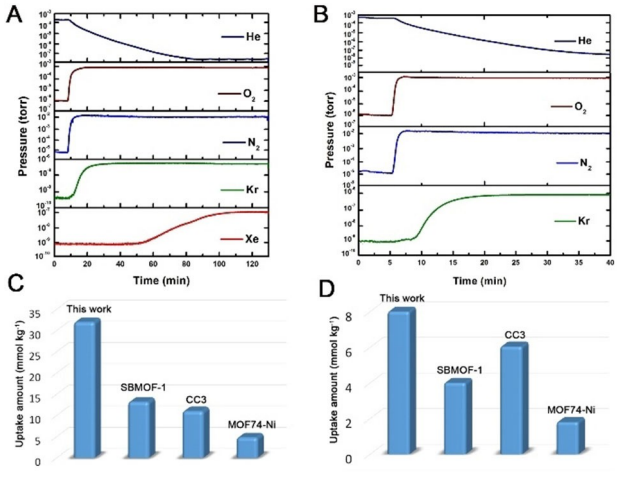

Figure 4. A) Column breakthrough experiment for 400 ppm Xe, 40 ppm Kr, 21 % O_2, balanced with N_2 at 298 K and 1 bar for ATC-Cu. B) Column breakthrough experiment for 1000 ppm Kr, 21 % O_2, balanced with N_2 at 298 K and 1 bar for ATC-Cu. C) Xe uptake amounts of top performance materials from column breakthrough experiment for 400 ppm Xe, 40 ppm Kr, 21 % O_2, balanced with N_2 at 298 K and 1 bar. D) Kr uptake amounts of top performance materials from column breakthrough experiment for 1000 ppm Kr, 21 % O_2, balanced with N_2 at 298 K and 1 bar.

that of Kr and other main gases in the air which indicates that ATC-Cu can effectively capture and separate Xe from a gas mixture useful for nuclear gas reprocessing. The Xe and Kr capacity of ATC-Cu from the breakthrough experiment is much higher than any MOFs and porous organic cage materials we tested thus far. As shown in Figure 4C, the equilibrium Xe capacity from breakthrough experiments in ATC-Cu (32 mmol kg^{-1}) surpassed any MOFs and porous organic cage materials we tested thus far. Further breakthrough experiments were performed on ATC-Cu to demonstrate the removal of Kr from the gas composition without Xe (1000 ppm Kr, 78 % N_2, and 21 % O_2) at room temperature (Figure 4B). The Kr capacity of Cu-ATC was found to be 8 mmol kg^{-1}, higher than the high-performance materials including NiMOF-74, CC3, and SBMOF-1 (Figure 4D).

In conclusion, we reported a self-adjusting framework in MOF for capturing trace Xe and Kr from the nuclear reprocessing off-gas. The self-adjusting behavior of ATC-Cu has been illustrated via gases-loaded SCXRD studies along with theoretical calculations. The unique self-adjusting framework endows the ATC-Cu the record Xe and Kr uptake capacity at 0.1 bar and 298 K, as well as the benchmark Xe capture capability in the nuclear reprocessing off-gas. This work provides a new route to design and implement novel porous materials with the self-adjusting framework for developing high-performance separation materials.

Acknowledgements

The authors thank the support from the Robert A. Welch Foundation (B-0027) and the US National Science Foundation (ECCS-2029800). Z. N. acknowledges the National Natural Science Foundation of China (Grant 22001186) and the National Science Foundation of Jiangsu Province (Grant BK20200853). T.P., K.A.F., and B.S. acknowledges the National Science Foundation (Award No. DMR-1607989), including support from the Major Research Instrumentation Program (Award No. CHE-1531590). Computational resources were made available by a XSEDE Grant (No. TG-DMR090028). Research Computing at the University of South Florida and High-Performance Computing at North Carolina State University. B.S. also acknowledges support from an ACS Petroleum Research Fund grant (ACS PRF 56673-ND6). PKT thank DOE—Office of Nuclear Energy for support. Particularly, we thank Sameh Elsaidi (PNNL), Mona Mohamed (PNNL), Ken Marsden (INL), John Vienna (PNNL), Patricia Paviet (PNNL) and Kimberly Gray (DOE NE). Partial support from the Researchers Supporting Program (RSP-2022/55) at King Saud University, Riyadh, Saudi Arabia is also acknowledged (A.M.A.).

Conflict of Interest

The authors declare no conflict of interest.

Data Availability Statement

The data that support the findings of this study are available from the corresponding author upon reasonable request.

Keywords: Gas Separation · Krypton · Metal–Organic Frameworks · Self-Adjusting · Xenon

[1] M. I. Hoffert, K. Caldeira, G. Benford, D. R. Criswell, C. Green, H. Herzog, A. K. Jain, H. S. Kheshgi, K. S. Lackner, J. S. Lewis, H. D. Lightfoot, W. Manheimer, J. C. Mankins, M. E. Mauel, L. J. Perkins, M. E. Schlesinger, T. Volk, T. M. L. Wigley, *Science* **2002**, *298*, 981–987.
[2] P. A. Kharecha, J. E. Hansen, *Environ. Sci. Technol.* **2013**, *47*, 4889–4895.
[3] Chu S. Majumdar, *Nature* **2012**, *488*, 294–303.
[4] J. P. Fontaine, F. Pointurier, X. Blanchard, T. Taffary, *J. Environ. Radioact.* **2004**, *72*, 129–135.
[5] a) B. Driehuys, J. Downward, *Science* **2006**, *314*, 432–433; b) N. P. Franks, R. Dickinson, S. L. M. de Sousa, A. C. Hall, W. R. Lieb, *Nature* **1998**, *396*, 324.
[6] S.-C. Hwang, W. R. Weltmer, *Helium Group Gases, Kirk-Othmer Encyclopedia of Chemical Technology*, Wiley, Hoboken, **2000**.
[7] F. G. Kerry, *Industrial Gas Handbook: Gas Separation and Purification*, CRC Press, Boca Raton, Florida, **2007**.
[8] a) J. Liu, P. K. Thallapally, D. Strachan, *Langmuir* **2012**, *28*, 11584–11589; b) P. Ryan, O. K. Farha, L. J. Broadbelt, R. Q. Snurr, *AIChE J.* **2011**, *57*, 1759–1766; c) A. Soleimani Dorcheh, D. Denysenko, D. Volkmer, W. Donner, M. Hirscher, *Microporous Mesoporous Mater.* **2012**, *162*, 64–68; d) H. Wang, K. Yao, Z. Zhang, J. Jagiello, Q. Gong, Y. Han, J. Li, *Chem. Sci.* **2014**, *5*, 620–624; e) M. H. Mohamed, S. K. Elsaidi, T. Pham, K. A. Forrest, H. T. Schaef, A. Hogan, L. Wojtas, W. Xu, B. Space, M. J. Zaworotko, P. K. Thallapally, *Angew. Chem. Int.*

Ed. **2016**, *55*, 8285–8289; *Angew. Chem.* **2016**, *128*, 8425–8429; f) T. Wang, Y.-L. Peng, E. Lin, Z. Niu, P. Li, S. Ma, P. Zhao, Y. Chen, P. Cheng, Z. Zhang, *Inorg. Chem.* **2020**, *59*, 4868–4873; g) L. Li, L. Guo, Z. Zhang, Q. Yang, Y. Yang, Z. Bao, Q. Ren, J. Li, *J. Am. Chem. Soc.* **2019**, *141*, 9358–9364; h) S. Xiong, Y. Gong, S. Hu, X. Wu, W. Li, Y. He, B. Chen, X. Wang, *J. Mater. Chem. A* **2018**, *6*, 4752–4758; i) H. Wang, Z. Shi, J. Yang, T. Sun, B. Rungtaweevoranit, H. Lyu, Y. B. Zhang, O. M. Yaghi, *Angew. Chem. Int. Ed.* **2021**, *60*, 3417–3421; *Angew. Chem.* **2021**, *133*, 3459–3463; j) K. B. Idrees, Z. Chen, X. Zhang, M. R. Mian, R. J. Drout, T. Islamoglu, O. K. Farha, *Chem. Mater.* **2020**, *32*, 3776–3782; k) H. Zhang, Y. Fan, R. Krishna, X. Feng, L. Wang, F. Luo, *Sci. Bull.* **2021**, *66*, 1073–1079; l) Z. Yan, Y. Gong, B. Chen, X. Wu, L. Cui, S. Xiong, S. Peng, *Sep. Purif. Technol.* **2020**, *239*, 116514; m) Y. Tao, Y. Fan, Z. Xu, X. Feng, R. Krishna, F. Luo, *Inorg. Chem.* **2020**, *59*, 11793–11800.

[9] a) D. Banerjee, A. J. Cairns, J. Liu, R. K. Motkuri, S. K. Nune, C. A. Fernandez, R. Krishna, D. M. Strachan, P. K. Thallapally, *Acc. Chem. Res.* **2015**, *48*, 211–219; b) L. Chen, P. S. Reiss, S. Y. Chong, D. Holden, K. E. Jelfs, T. Hasell, M. A. Little, A. Kewley, M. E. Briggs, A. Stephenson, K. M. Thomas, J. A. Armstrong, J. Bell, J. Busto, R. Noel, J. Liu, D. M. Strachan, P. K. Thallapally, A. I. Cooper, *Nat. Mater.* **2014**, *13*, 954–960.

[10] a) X. Chen, A. M. Plonka, D. Banerjee, R. Krishna, H. T. Schaef, S. Ghose, P. K. Thallapally, J. B. Parise, *J. Am. Chem. Soc.* **2015**, *137*, 7007–7010; b) D. Banerjee, C. M. Simon, A. M. Plonka, R. K. Motkuri, J. Liu, X. Chen, B. Smit, J. B. Parise, M. Haranczyk, P. K. Thallapally, *Nat. Commun.* **2016**, *7*, 11831.

[11] a) C. A. Fernandez, J. Liu, P. K. Thallapally, D. M. Strachan, *J. Am. Chem. Soc.* **2012**, *134*, 9046–9049; b) H. Wang, M. Warren, J. Jagiello, S. Jensen, S. K. Ghose, K. Tan, L. Yu, T. J. Emge, T. Thonhauser, J. Li, *J. Am. Chem. Soc.* **2020**, *142*, 20088–20097.

[12] B. Chen, M. Eddaoudi, T. M. Reineke, J. W. Kampf, M. O'Keeffe, O. M. Yaghi, *J. Am. Chem. Soc.* **2000**, *122*, 11559–11560.

[13] Deposition numbers 2123674 (Xe loaded ATC-Cu) and 2123675 (Kr loaded ATC-Cu) contain the supplementary crystallographic data for this paper. These data are provided free of charge by the joint Cambridge Crystallographic Data Centre and Fachinformationszentrum Karlsruhe Access Structures service.

[14] a) Z. Niu, X. Cui, T. Pham, P. C. Lan, H. Xing, K. A. Forrest, L. Wojtas, B. Space, S. Ma, *Angew. Chem. Int. Ed.* **2019**, *58*, 10138–10141; *Angew. Chem.* **2019**, *131*, 10244–10247; b) Z. Niu, X. Cui, T. Pham, G. Verma, P. C. Lan, C. Shan, H. Xing, K. A. Forrest, S. Suepaul, B. Space, A. Nafady, A. M. Al-Enizi, S. Ma, *Angew. Chem. Int. Ed.* **2021**, *60*, 5283–5288; *Angew. Chem.* **2021**, *133*, 5343–5348.

Manuscript received: December 30, 2021
Accepted manuscript online: January 12, 2022
Version of record online: January 27, 2022